Nanosolvation

DOI: 10.1002/anie.201301667

Nanosolvation-Induced Stabilization of a Protonated Peptide Dimer Isolated in the Gas Phase**

Aleksandar R. Milosavljević, Viktor Z. Cerovski, Francis Canon, Laurent Nahon, and Alexandre Giuliani**

The structure and functionality of biomolecules are intrinsically linked with their aqueous environment. There has been a long-standing effort to understand the effect of the surrounding water solvation shell on the conformation of biomolecules and how it influences both their functional properties and susceptibility to external factors (such as ionizing radiation).[1–7] The structure–function paradigm postulates that proteins are required to adopt a specific folding to be biologically active.[8] Therefore, continuous intensive research has been devoted to protein folding and how the active native state is adopted.[9] Weak molecular interactions have been proposed to have a major role in protein folding and in the formation of macromolecular complexes.[10] Thus, understanding how the structure of complexes is determined and stabilized is a crucial issue. In particular, the solvent has a key role in self-assembling processes.[11]

The need to gain a deeper understanding of the effect of water solvation on the protein structure and the ability of mass spectrometry to study isolated intact non-covalent complexes even from heterogeneous mixtures,[12] have led to an intensive investigation of gradual solvation of biomolecules (Ref. [1–7] and references therein). The limit of the so-called microsolvation (or nanosolvation), referring to only a small and well-defined number of attached water molecules, has been conceived. For example, it has been shown recently that even a single or a few water molecules can significantly affect a chemical reaction dynamics[5,6] or the peptide structure.[7]

Herein we report a comparative experimental and theoretical study on protonated leucine–enkephalin (Leu-Enk: YGGFL) peptide dimer ion and on the same system solvated with three water molecules. Leu-Enk has turned into a standard model in mass spectrometry,[13] and is used here as a model system for peptide–peptide interactions. This model is pertinent not only for non-covalent complex formation but also for the acquisition of secondary and ternary structures of proteins. Nanosolvation of a fragile biomolecular complex by only a few water molecules appears to have a dramatic impact on its stability. We have compared the photon-induced fragmentation in the vacuum ultraviolet (VUV) of a bare and a solvated protonated Leu-Enk peptide dimer ion isolated in the gas phase, and found a drastic reduction of the fragmentation abundance of the solvated precursor. Furthermore, the increased stability that is due to nanosolvation was substantiated by detecting the dication produced upon photoionization of the hydrated protonated species $[2\,\text{Leu-Enk} + 3\,H_2O + H]^+$, which can be preserved in the gas phase, thus also allowing a precise measurement of the ionization threshold of 8.53 ± 0.050 eV. Theoretical study of the structure of the nanosolvated peptide dimer is consistent with the experimental findings. The calculations show that hydration with only 3 water molecules does not affect significantly the 3D structure of the dimer, but rather stabilizes it by about 1.5 eV.

Figure 1 shows tandem mass spectra (MS^2) recorded after VUV irradiation at 9 eV photon energy of isolated $[2\,\text{Leu-Enk} + H]^+$ (m/z 1111) and $[2\,\text{Leu-Enk} + 3\,H_2O + H]^+$ (m/z 1165) precursor ions. Additional mass spectra recorded at lower photon energy are given in the Supporting Information. The single VUV photon absorption by the bare protonated peptide dimer $[2\,\text{Leu-Enk} + H]^+$ (Figure 1 a) clearly produces abundant dissociations of the precursor into monomer units. The abundance of the monomer cation $[\text{Leu-Enk} + H]^+$ at 9 eV photon energy is as large as 48% relative to the precursor, a lower limit owing to possible photon reabsorption during the irradiation time. Careful observation of the isotopic distribution of the m/z 556 ion (Figure 1 a, inset) does not reveal any sign of the $[2\,\text{Leu-Enk} + H]^{\bullet 2+}$ radical dication (expected at m/z 555.5) produced by photoionization (PI) of the precursor, as the photon energy of 9 eV is above the ionization threshold.[14] Photoabsorption is also accompanied by cleavage of the peptide backbone into sequence ions and neutral losses from the precursor and the monomer, which is similar to previous results.[14] The photoinduced fragmentation of the microsolvated isolated dimer precursor [2 Leu-

[*] Dr. A. R. Milosavljević, Dr. V. Z. Cerovski
Institute of Physics Belgrade, University of Belgrade
Pregrevica 118, 11080 Belgrade (Serbia)
E-mail: vraz@ipb.ac.rs
Dr. F. Canon
INRA, UMR1324 Centre des Sciences du Goût et de l'Alimentation
21000 Dijon (France)
Dr. L. Nahon, Dr. A. Giuliani
Synchrotron SOLEIL, L'Orme des Merisiers, Saint Aubin
91192 Gif-sur-Yvette (France)
E-mail: alexandre.giuliani@synchrotron-soleil.fr
Dr. A. Giuliani
UAR 1008 CEPIA, INRA
44316 Nantes (France)

[**] This work was supported by the Agence Nationale de la Recherche Scientifique, France, under the project no. ANR-08-BLAN-0065 and partially by "Pavle Savic" project of bilateral scientific collaboration between Serbia and France and the COST Action MP1002 (Nano-IBCT). A.R.M. and V.Z.C. acknowledge support by the MESTD RS (Project Nos. 171020 and 171033, respectively). The SOLEIL synchrotron radiation facility is acknowledged for providing beamtime under project 20110694.

Supporting information for this article is available on the WWW under http://dx.doi.org/10.1002/anie.201301667.

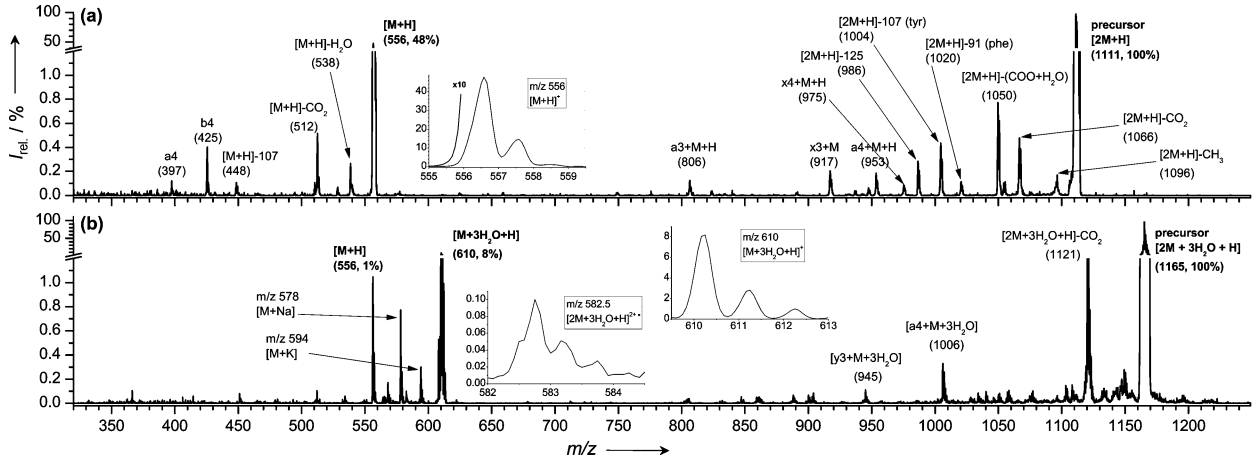

Figure 1. Photoactivation tandem mass spectra of leucine-enkephalin (Leu-Enk) peptide dimer recorded after irradiation of a) $[2\,\text{Leu-Enk}+\text{H}]^+$ and b) $[2\,\text{Leu-Enk}+3\,\text{H}_2\text{O}+\text{H}]^+$ precursors at 9 eV photon energy. Insets: a close up of the mass regions around $[\text{Leu-Enk}+\text{H}]^+$ (m/z 556), $[\text{Leu-Enk}+3\,\text{H}_2\text{O}+\text{H}]^+$ (m/z 610), and $[2\,\text{Leu-Enk}+3\,\text{H}_2\text{O}+\text{H}]^{2+}$ (m/z 582.5) charge states.

$\text{Enk}+3\,\text{H}_2\text{O}+\text{H}]^+$ (Figure 1b) appears to be drastically different from that of the bare species (Figure 1a). First, the comparison of the two mass spectra shows that the presence of only three water molecules on the dimer strongly decreases the abundances of all of the product ions under identical experimental conditions. Particularly, the strongest dissociation channel, corresponding again to the dissociation into monomer units, produces only up to 8% abundance of $[\text{Leu-Enk}+3\,\text{H}_2\text{O}+\text{H}]^+$ (m/z 610) and about 1% of $[\text{Leu-Enk}+\text{H}]^+$ (m/z 556). It is worth noting that the hydrated protonated monomer (Figure 1b; bound to the three water molecules) is more abundant than its dehydrated counterpart.

It appears that, phenomenologically, the microsolvation of the protonated Leu-Enk dimer with only three water molecules provide a very efficient shielding against VUV induced dissociation and backbone fragmentation. Indeed, the fragmentation pattern corresponding to backbone fragments of bare dimer (Figure 1a) is practically not observed for the hydrated species (Figure 1b). Actually, the second most abundant fragmentation channel for the microsolvated precursor corresponds to the loss of CO_2. It is interesting to note that CO_2 loss was also the only relatively intensive fragmentation channel upon both valence[15] and inner-shell[16] PI of protein ions. Finally, in contrast to the case of the bare dimer, the doubly charged cation $[2\,\text{Leu-Enk}+3\,\text{H}_2\text{O}+\text{H}]^{\bullet 2+}$, formed upon PI of the microsolvated precursor, can be traced down in the recorded MS^2 spectrum. Although of low abundance, the signal-to-noise ratio is high enough to clearly distinguish the peak at the exactly expected m/z 582.5 and with an isotopic distribution explicitly indicating a doubly charged ion (see insets in Figure 1b).

Geometries of the lowest energy conformers found of hydrated dimer (CF_1) $[2\,\text{Leu-Enk}+3\,\text{H}_2\text{O}+\text{H}]^+$ and of the corresponding bare one (CF_1') $[2\,\text{Leu-Enk}+\text{H}]^+$, obtained by molecular dynamics (MD) and 6-31+G(d,p) density functional theory (DFT) calculations, are shown in Figure 2. The quantitative results are as following: vertical ionization energies (VIE) of CF_1 (hydrated) and CF_1' (bare) are 9.28 eV and 9.31 eV, respectively; binding energy of CF_1 (E_{int}) is 206.9 kJ mol^{-1}; binding energy of CF_1' (E_{int}') is 67.4 kJ mol^{-1}; the difference between binding energies ($E_{int}-E_{int}'$) is 139.5 kJ mol^{-1} (1.45 eV). The geometries of four lowest energy hydrated conformers are compared to the bare species in the Supporting Information. In all cases, the dimer forms a bound state both with and without water molecules. However, comparison of the bare and hydrated complexes reveals that the binding is strongly enhanced upon

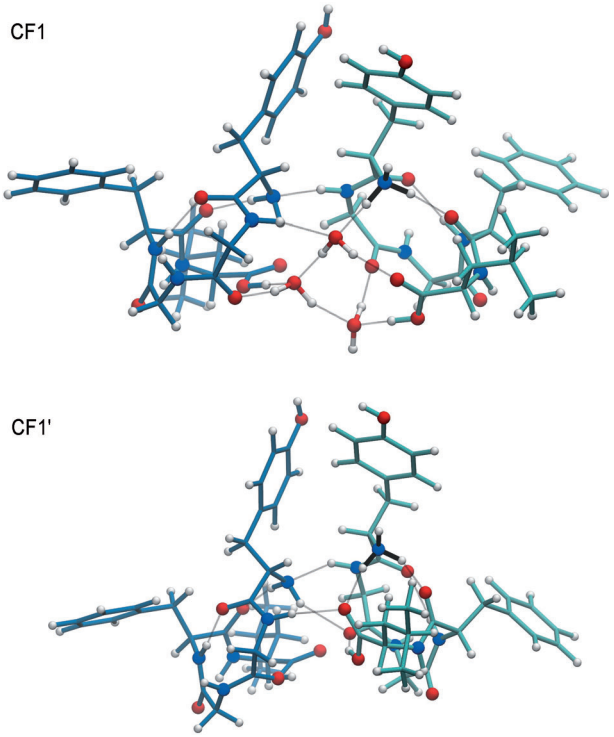

Figure 2. B3LYP/6-31+G(d,p) optimized geometry of the lowest energy CF_1 conformer found of $[2\,\text{Leu-Enk}+3\,\text{H}_2\text{O}+\text{H}]^+$ and the corresponding bare dimer CF_1' $[2\,\text{Leu-Enk}+\text{H}]^+$. Thin gray lines represent H-bonds; black lines denote NH_3 group.

nanosolvation (ca. 1.5 eV for CF_1). This is due to the flexibility of H_2O to adjust its position and orientation with respect to the other molecules, thus increasing the effective number of H-bonds between monomers. Without water, the dimer structure is very similar and H-bonding also exists, but the active sites are much less flexible to adjust, as their positions are determined primarily by their position and orientation within the CF of the monomer to which they belong.

It should be noted that the present experimental observations support the calculated lowest-energy dimer geometries. The isolated a_4- and b_4-sequence ions observed in the tandem mass spectra at 7.2 eV photon energy (Supporting Information, Figure S1) of the bare dimer indicate that the proton is located on the N-terminal nitrogen. Furthermore, a hypothetical linear dimer arrangement does not fit with the observation of both N-terminal and C-terminal fragments in association with the monomer (a_3+M, a_4+M+H, x_3+M, x_4+M+H). These findings suggest a bare dimer formed by two peptides associated in a parallel stacking manner and protonated on one of N-terminal nitrogen atoms, as indeed found theoretically. On the other hand, the fragmentation pattern of the nanosolvated dimer is scarce and dominated by peptide fragments associated with the monomer and preserving all three water molecules. The latter observation suggests that the water molecules are shared between the two monomers that is, are located at their interface within the complex, preferably linked together close to the charge, and thus remain attached to the observed protonated monomer. Such an arrangement is indeed obtained in most of the calculated geometries.

The apparent increased stability toward VUV of the hydrated complex with respect to the bare species is striking and questions the energy dissipation process. Irradiation at energies above the ionization energy (IE) produces a radical cation and an electron, carrying away part of the energy as kinetic energy. However, even below the IE, nanosolvation produces a frustrated dissociation in the dimer. Our tentative explanation is that the precursor may still undergo the photofragmentation, where the fragments would remain attached to the rest of the complex and be thus hidden to our measurements. Similar observations have been made under ECD or ETD conditions, leading to so-called EC-no-D or ET-no-D products.[17] Additionally, the precursor may undergo a photoisomerization. However, we cannot exclude some other complementary radiationless relaxation mechanisms that would produce a fast deactivation of the excited molecule.[18]

Additional experimental evidence of the increased stability of hydrated dimer comes from the PI partial ion yields obtained by recording MS^2 as a function of the photon energy. Relative abundance of a specific peak (obtained by integration over the isotopic distribution) is then normalized to both the photon flux and the total ionic current.[15] The yield of the $[2\,\text{Leu-Enk}+3\,H_2O+H]^{2+\bullet}$ product ion from the hydrated precursor shows a clear threshold behavior (Figure 3a), confirming that it is formed by the PI process: $[2\,\text{Leu-Enk}+3\,H_2O+H]^{+}+h\nu\rightarrow[2\,\text{Leu-Enk}+3\,H_2O+H]^{2+\bullet}+e^{-}$. Fitting the experimental PI efficiency curve by a Wannier-type

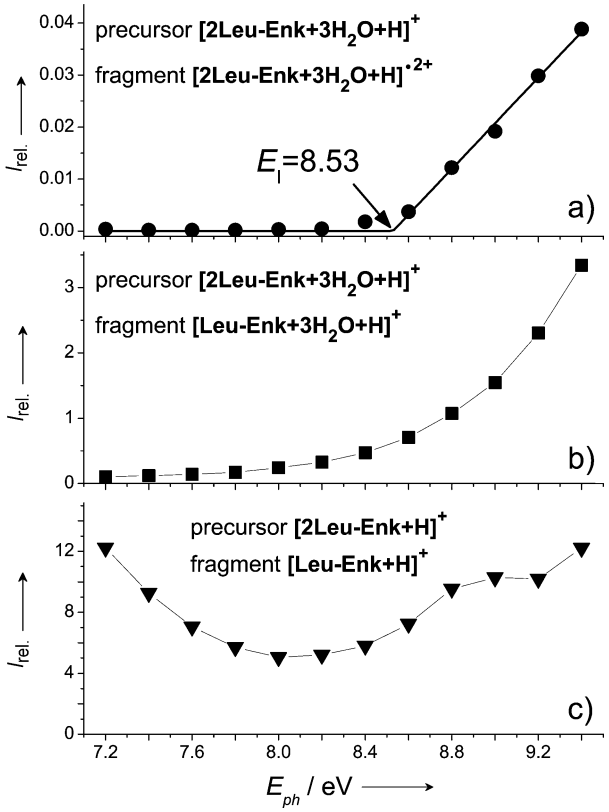

Figure 3. Photoionization yields of a) $[2\,\text{Leu-Enk}+3\,H_2O+H]^{\bullet 2+}$ (m/z 582.25–584.0), b) $[\text{Leu-Enk}+3\,H_2O+H]^{+}$ (m/z 609.5–613.0), and c) $[\text{Leu-Enk}+H]^{+}$ (m/z 555.5–559.0) fragments. The full line in (a) represents the linear Wannier fit.

threshold function[19,20] allows a precise determination of the IE of the microsolvated protonated Leu-Enk dimer of 8.53 ± 0.050 eV. Note that the latter value represents the adiabatic ionization energy (AIE)[20] rather than VIE obtained theoretically. The present calculations predict that all hydrated conformers have their HOMO localized on the tyrosine end of the non-protonated monomer (see Supporting Information). However, the higher calculated value of VIE for CF_1 in comparison with VIE of tyrosine, confirms that electrons from the HOMO are more strongly bound in the protonated hydrated dimer than in the neutral tyrosine, despite similar location and nodal structure of the two HOMOs. This increase in IE arises from the positive charge of the ion.[20] The VIE for tyrosine, calculated by MP2, was recently reported at 8.53 eV,[21] while in the present work we calculate that tyrosine in the lowest-energy CF[21] optimized at B3LYP/cc-pVQZ level of DFT has VIE = 8.27 eV.

At photon energies above the ionization threshold a radical doubly charged ion is formed, thus an appearance of a new positive charge on the protonated complex creates a Coulombic repulsion. A simple estimation of the Coulomb energy ($e^2/4\pi\varepsilon R$), which should be counteracted by microsolvation to prevent the dissociation of the system, is obtained from our calculated distance ($R\approx0.6$ nm) between the center of the tyrosine ring and the protonated nitrogen in CF_1 to be

about 2.4 eV (taking $\varepsilon = \varepsilon_0$, the permittivity of vacuum). The later estimation is an upper limit and in fair agreement with the calculated binding energy of the solvated complex (ca. 1.5 eV), explaining the experimental observation of the doubly charged hydrated parent ion.

An evidence of the retention of the fragments inside the complex by water molecules also comes from the comparison of the energy dependence for dissociation into monomers of the bare and hydrated Leu-Enk (Figure 3b,c). The relative yield of ions in Figure 3c shows an important contribution from photons below the ionization threshold, which corresponds to photodissociation occurring from electronic excited states of the precursor. In this scenario, relaxation of electronic excited states leads to redistribution of energy among the vibrational degrees of freedom, leading to the dissociation of the non-covalent complex from the hot ground state. Dissociation into monomers for the hydrated dimer, on the other hand, strongly increases only above the ionization threshold. It should be noted that such a drastic stabilization of the hydrated dimer cannot be due to a small (about 6%) increase of degrees of freedom by adding 3 water molecules to the system.

In summary, the present results clearly demonstrate a significant effect of nanosolvation-induced stabilization of a peptide dimer isolated in the gas phase. The theoretical analysis indicates a generic binding mechanism induced by only a few water molecules bridging the monomers and enhancing the stability of the complex (by about 1.5 eV), without a significant influence on its 3D arrangement. This is an important point to consider when stability of protein noncovalent complexes and protein structure is assessed for isolated unhydrated ions, by mass spectrometry for example.[12] Moreover, the phenomenologically shielding effect of microsolvation observed here is of interest in the field of radiation damage and could help in the future to have a better understanding of these processes at the molecular level (see Ref. [22] and references therein).

Methods

The experimental setup is based upon a commercial linear quadrupole ion trap mass spectrometer (Thermo Finnigan LTQ XL), which was connected to the VUV beamline DESIRS[23] of the SOLEIL storage ring (France).[24] The ions are produced by an electrospray ionization (ESI) source and introduced into the trap from the front side of the spectrometer. After the isolation of a desired precursor, $[2\,\text{Leu-Enk} + \text{H}]^+$ or $[2\,\text{Leu-Enk} + 3\,\text{H}_2\text{O} + \text{H}]^+$, the monochromatized synchrotron beam was sent directly into the trap from the back side during a 500 ms timeframe. After irradiation, MS^2 spectra were recorded as a function of the photon energy (more details can be found in Ref.[24]). In the present study, the protonated Leu-Enk (Sigma Aldrich) molecules were generated by the ESI source from water/MeCN (75:25) solution at 10 μM. The hydrated clusters produced from the ESI source were preserved by tuning an appropriate combination of parameters, such as the concentration of the solution, transfer tube temperature, voltages, and sheath gas flow rate.

The theoretical modeling was done starting with the two lowest energy geometries of Leu-Enk from Ref. [25], where about 70 dimer geometries with and without water molecules have been studied. Among such obtained candidates for $[2\,\text{Leu-Enk} + \text{H} + 3\,\text{H}_2\text{O}]^+$, four with the lowest energy were simulated at B3LYP/6–31G(d) level of DFT using nwchem.[26] The first step was the full geometrical relaxation, followed by calculation of VIE and binding energy of monomers, E_{int}, which includes corrections that are due to the basis-set superposition error.[27] The conformers with the lowest energy were then optimized without $3\,\text{H}_2\text{O}$, and their binding energy, E_{int}', was calculated. Finally, all hydrated conformers, as well as the lowest energy bare conformer, were simulated at 6-31 + G(d,p) level of DFT.

Received: February 26, 2013
Revised: April 5, 2013
Published online: June 6, 2013

Keywords: ion spectroscopy · mass spectrometry · microsolvation · photoionization · radiation damage

[1] D. Liu, T. Wyttenbach, P. E. Barran, M. T. Bowers, *J. Am. Chem. Soc.* **2003**, *125*, 8458.
[2] A. Kamariotis, O. V. Boyarkin, S. R. Mercier, R. D. Beck, M. F. Bush, E. R. Williams, T. R. Rizzo, *J. Am. Chem. Soc.* **2006**, *128*, 905.
[3] J. S. Prell, T. M. Chang, J. T. O'Brien, E. R. Williams, *J. Am. Chem. Soc.* **2010**, *132*, 7811.
[4] H. S. Biswal, Y. Loquais, B. Tardivel, E. Gloaguen, M. Mons, *J. Am. Chem. Soc.* **2011**, *133*, 3931.
[5] R. Otto, J. Brox, S. Trippel, M. Stei, T. Best, R. Wester, *Nat. Chem.* **2012**, *4*, 534.
[6] K. Doi, E. Togano, S. S. Xantheas, R. Nakanishi, T. Nagata, T. Ebata, Y. L. Inokushi, *Angew. Chem.* **2013**, *125*, 4476; *Angew. Chem. Int. Ed.* **2013**, *52*, 4380.
[7] N. S. Nagornova, T. R. Rizzo, O. V. Boyarkin, *Science* **2012**, *336*, 320.
[8] C. B. Anfinsen, *Science* **1973**, *181*, 223.
[9] A. I. Bartlett, S. E. Radford, *Nat. Struct. Mol. Biol.* **2009**, *16*, 582.
[10] A. C. Gavin, *Expert Rev. Proteomics* **2005**, *2*, 291.
[11] M. H. Jacob, C. Saudan, G. Holtermann, A. Martin, D. Perl, A. E. Merbach, F. X. Schmid, *J. Mol. Biol.* **2002**, *318*, 837.
[12] F. Canon, R. Ballivian, F. Chirot, R. Antoine, P. Sarni-Manchado, J. Lemoine, P. Dugourd, *J. Am. Chem. Soc.* **2011**, *133*, 7847.
[13] J. Sztáray, A. Memboeuf, L. Drahos, K. Vékey, *Mass Spectrom. Rev.* **2011**, *30*, 298.
[14] S. Bari, O. Gonzalez-Magana, G. Reitsma, J. Werner, S. Schippers, R. Hoekstra, T. Schlatholter, *J. Chem. Phys.* **2011**, *134*, 024314.
[15] A. R. Milosavljević, C. Nicolas, J. Lemaire, C. Déhon, R. Thissen, J.-M. Bizau, M. Réfrégiers, L. Nahon, A. Giuliani, *Phys. Chem. Chem. Phys.* **2011**, *13*, 15432.
[16] A. R. Milosavljević, F. Canon, C. Nicolas, C. Miron, L. Nahon, A. Giuliani, *J. Phys. Chem. Lett.* **2012**, *3*, 1191.
[17] a) A. R. Ledvina, G. C. McAlister, M. W. Gardner, S. I. Smith, J. A. Madsen, J. C. Schwartz, G. C., Jr. Stafford, J. E. P. Syka, J. S. Brodbelt, J. J. Coon, *Angew. Chem.* **2009**, *121*, 8678; *Angew. Chem. Int. Ed.* **2009**, *48*, 8526; b) D. M. Horn, K. Breuker, A. J. Frank, F. W. McLafferty, *J. Am. Chem. Soc.* **2001**, *123*, 9792.
[18] W. Domcke, A. L. Sobolewski, *Nat. Chem.* **2013**, *5*, 258.
[19] G. H. Wannier, *Phys. Rev.* **1953**, *90*, 817.
[20] A. Giuliani, A. R. Milosavljević, C. Hinsen, F. Canon, C. Nicolas, M. Réfrégiers, L. Nahon, *Angew. Chem.* **2012**, *124*, 9690; *Angew. Chem. Int. Ed.* **2012**, *51*, 9552.
[21] D. Close, *J. Phys. Chem. A* **2011**, *115*, 2900.
[22] M. Smyth, J. Kohanoff, *J. Am. Chem. Soc.* **2012**, *134*, 9122.
[23] L. Nahon, N. de Oliveira, G. Garcia, J. F. Gil, B. Pilette, O. Marcouille, B. Lagarde, F. Polack, *J. Synchrotron Radiat.* **2012**, *19*, 508.

[24] A. R. Milosavljević, C. Nicolas, J.-F. Gil, F. Canon, M. Réfrégiers, L. Nahon, A. Giuliani, *J. Synchrotron Radiat.* **2012**, *19*, 174.
[25] N. C. Polfer, J. Oomens, S. Suhai, B. Paizs, *J. Am. Chem. Soc.* **2007**, *129*, 5887.
[26] M. Valiev, E. J. Bylaska, N. Govind, K. Kowalski, T. P. Straatsma, H. J. J. Van Dam, D. Wang, J. Nieplocha, E. Apra, T. L. Windus, W. A. de Jong Valiev, *Comput. Phys. Commun.* **2010**, *181*, 1477.
[27] S. S. Xantheas, *J. Chem. Phys.* **1996**, *104*, 8821.

